



RESEARCH PAPER



Functional characterization of the Glyoxalase-I (*PdGLX1*) gene family in date palm under abiotic stresses

Gerry Aplang Jana  and Mahmoud W. Yaish 

Department of Biology, College of Sciences, Sultan Qaboos University, Muscat, Oman

ABSTRACT

Methylglyoxal (MG), a cytotoxic oxygenated short aldehyde, is a by-product of various metabolic reactions in plants, including glycolysis. The basal level of MG in plants is low, whereby it acts as an essential signaling molecule regulating multiple cellular processes. However, hyperaccumulation of MG under stress conditions is detrimental for plants as it inhibits multiple developmental processes, including seed germination, photosynthesis, and root growth. The evolutionarily conserved glyoxalase system is critical for MG detoxification, and it comprises of two-enzymes, the glyoxalase-I and glyoxalase-II. Here, we report the functional characterization of six putative glyoxalase-I genes from date palm (*Phoenix dactylifera* L.) (*PdGLX1*), by studying their gene expression under various environmental stress conditions and investigating their function in bacteria (*Escherichia coli*) and yeast (*Saccharomyces cerevisiae*) mutant cells. The putative *PdGLX1* genes were initially identified using computational methods and cloned using molecular tools. The *PdGLX1* gene expression analysis using quantitative PCR (qPCR) revealed differential expression under various stress conditions such as salinity, oxidative stress, and exogenous MG stress in a tissue-specific manner. Further, *in vivo* functional characterization indicated that overexpression of the putative *PdGLX1* genes in *E. coli* enhanced their growth and MG detoxification ability. The putative *PdGLX1* genes were also able to complement the loss-of-function MG hypersensitive GLO1 (YML004C) yeast mutants and promote growth by enhancing MG detoxification and reducing the accumulation of reactive oxygen species (ROS) under stress conditions as indicated by flow cytometry. These findings denote the potential importance of *PdGLX1* genes in MG detoxification under stress conditions in the date palm.

ARTICLE HISTORY

Received 7 July 2020
Revised 12 August 2020
Accepted 14 August 2020

KEYWORDS

Functional characterization; glyoxalase-I; date palm; methylglyoxal; ROS; salinity

Introduction

Plants being sessile organisms are directly affected by various abiotic and biotic factors, which determine their growth and development, thereby affecting the potential yields of crop plants.^{1,2} Date palm (*Phoenix dactylifera* L.) is a monocotyledon, dioecious plant, which is an important socioeconomic and abiotic stress-tolerant plant mainly grown in the hot and arid regions of the middle east and north Africa.³ Currently, this tree is suffering excessive salinity, which may be attributed to many environmental factors such as lack of precipitation, overexploitation of underground water, high evaporation rate, and the rising sea levels brought about by climate change.⁴ To overcome the adverse effects of stress conditions, plants have developed multiple mechanisms to alter their morphological, physiological, biochemical, and molecular processes.^{5–7} These alterations help in reducing the stress, thereby enabling the plants to grow and develop under various adverse environmental conditions.⁸ A vast number of plant-stress interaction pathways have been reported to be involved in stress tolerance and adaptation.⁹ Interestingly, it has been noted that various stress conditions lead to the accumulation of toxic aldehydes, of which methylglyoxal (MG), an α , β -dicarbonyl ketoaldehyde by-product of various metabolic processes, acts as an essential signaling molecule,¹⁰ and functions as a Hill oxidant and catalyzes the photoreduction of O₂ to

superoxide (O₂⁻) in the photosystem-I.¹¹ Therefore, MG could be used as a biomarker for plant stress tolerance.¹²

It has been previously reported that there is a 2- to 6- fold increase in the accumulation of MG in response to various stress.¹³ This increase leads to an upregulation in the reactive oxygen species (ROS) production, a decrease in the glutathione (GSH) levels and a disruption in the antioxidant enzyme function in plants.^{8,14} Various works have shown that MG regulatory function is governed in a concentration-dependent manner, whereby a lower concentration (0.1 mM) of MG did not inhibit germination but inhibited root elongation, however, at a higher concentration (1 mM MG) it inhibited seed germination in Arabidopsis.¹⁵ It was also observed that exogenous application of MG in Arabidopsis at a lower concentration (≤ 1 mM) induced stomatal closure via an extracellular oxidative burst and an elevation of [Ca²⁺]_{cyt} without reducing the viability of guard cells, however, at a higher concentration (≥ 1 mM), MG was cytotoxic.¹⁶ In addition, MG has also been shown to prevent light-induced stomatal opening by inhibiting inward potassium (K⁺) channels into the guard cells of Arabidopsis.¹⁶ A gene chip microarray analysis of rice plants exposed to 10 mM MG revealed that 966 genes were upregulated, and 719 genes were down-regulated, of which 18% and 14% are genes related to signal transduction, respectively.¹⁷ These findings indicate a regulatory role of MG on signal

transduction, thus signifying its possible involvement in plant stress signaling.

Further, MG has also been reported to inactivate the anti-oxidant enzyme, cytosolic ascorbate peroxidase (NtcAPX) in *Nicotiana tabacum* by modification of the amino acids of the enzyme.¹⁸ Therefore, to prevent the hyperaccumulation of MG in the cell under stress conditions, various detoxification pathways are involved in MG breakdown,¹⁹ of which the universally conserved glyoxalase system is the most efficient.²⁰ Within the glyoxalase pathway, MG, along with GSH is first non-enzymatically converted to hemithioacetate, after which the enzyme glyoxalase-I (also known as lactoylglutathione lyase) catalyzes the breakdown to S-lactoylglutathione. The glyoxalase-II further hydrolyzes S-lactoylglutathione to D-lactate and recycles GSH. The MG-scavenging glyoxalase pathway is believed to have diverse physiological functions in the plant. However, its role in stress tolerance is the most widely studied.²¹ In addition, various reports have observed an increase in the expression of the MG detoxification glyoxalase genes in plants under stress conditions, thus suggesting that these enzymes play an essential role in the plant's stress adaptation.^{22–25} Furthermore, transgenic overexpression of the MG-detoxification glyoxalase enzymes has been shown to enhance tolerance to various stress conditions and also to lower MG levels in the plants.^{26–29}

The aim of this project was to functionally characterize glyoxalase-I (EC 4.4.1.5) genes encoded by the date palm genome (*PdGLX1*), study their expression profile under various stress conditions, and determine their function in *E. coli* and GLO1 knockout yeast cells using a functional complementation assay. Here, we report six putative *PdGLX1* genes in the genome of the date palm, namely *PdGLX1:1*, *PdGLX1:2*, *PdGLX1:3*, *PdGLX1:4*, *PdGLX1:5*, and *PdGLX1:6*. The expression of these genes varies under various stress treatments suggesting that their expression is induced in a stress-dependent manner. Further, heterologous expression of the *PdGLX1* in BL21 (DE3) *E. coli* and yeast mutant cells enhanced stress tolerance and significantly reduced MG accumulation in the cells. Our research highlights the importance of the *PdGLX1* gene family in stress tolerance in date palm.

Materials and methods

Plant growth conditions and treatments

Date palm seeds (cv. *Khalas*) were soaked overnight in distilled water at 37°C. Debris was washed away from the seeds with tap water. A 70% ethanol solution was then used to surface-sterilize the seeds, followed by rinsing them twice using sterile distilled water. The seeds were then germinated at 37°C on moist sterile vermiculite for ten days as previously described.^{30,31} The germinated seedlings were potted in multi-purpose compost (Bulrush Horticulture Ltd, UK). The pots were maintained in the greenhouse at 30°C, 350 $\mu\text{mol.m}^{-2}.\text{s}^{-1}$ light intensity and a photoperiod of 16 h/8 h light/dark cycle. The pots were irrigated on a weekly basis with distilled water to field capacity for about three weeks. Subsequently, the pots were segregated according to the irrigation solutions (treatments): control (distilled water), salt stress (300 mM NaCl),

oxidative stress (10 mM H₂O₂), and MG stress (10 mM MG). The plants were harvested after six weeks of treatment.

The concentration of the NaCl and MG used in the following experiments was selected empirically. The highest non-lethal level the NaCl and MG was selected to trigger the tolerance/detoxification process in the used cells. In general, the proper highest concentration used in these experiments was the one which can significantly affect the growth of the wildtype organism but did not show a negative effect on the transgenic microorganisms used in this project. The date palm, as well as yeast cells, are NaCl tolerant organisms by nature; however, bacteria cells are less tolerant; therefore, a lower concentration of NaCl was used in the corresponding experiments.

Identification of *GLYOXALASE-I* genes (*PdGLX1*) within *P. dactylifera* L. genome

The *GLYOXALASE-I* specific amino acid domain was retrieved from the protein families (Pfam) database and used as a probe for the protein sequence search (KLKNPMLVVTIDIDKSVEFYKVKVFLYVIMDFGANKTLT-GGLALQTSETYKEFIGTSDISFGGNNFEVYFEEEDFDKFA-DRLKEYDIEYVHPHIIHSWGQRVRFYDPDKHIIIEV). The BLASTP search tool was then used against the date palm genome (taxid:42345), previously deposited within the National Center for Biotechnology Information (NCBI) database, to identify putative *PdGLX1* proteins, which were then analyzed using the Hidden Markov Model (HMM) profile on the Pfam database.³²

In silico analysis and subcellular localization prediction of *PdGLX1*

Computational and biochemical analyses, in addition to subcellular localization prediction, were performed to understand the function of the *PdGLX1* proteins in date palm. The pI/MW tool on the ExPASy platform was used to determine the theoretical molecular weight (MW) and the isoelectric point (pI).³³ Three subcellular localization prediction tools were utilized with default search parameters: the Wolf PSORT,³⁴ the CELLO v.2.5,³⁵ and the ChloroP localization tools.³⁶ The presence of *cis*-acting elements within 1.5 kb of the deduced promoter region was determined using PlantCARE.³⁷ The coding region from the genomic DNA was verified using the GSDS 2.0 tool.³⁸ The Multiple Expectation for Motif Elicitation (MEME) tool was utilized for conserved motif prediction using default parameters.³⁹ The phylogenetic relationship between *PdGLX1* and other protein orthologues of *Arabidopsis thaliana*, *Medicago sativa*, *Oryza sativa*, *Glycine max*, and *Sourgum bicolor* was constructed using the neighbor-joining method and Kimura 2-parameter model implemented within the MEGAX software.⁴⁰

Cloning of the putative *PdGLX1* genes

Total RNA from date palm leaf and root samples was isolated using the MRIP method.⁴¹ SuperScript IV Reverse Transcriptase (Invitrogen, California, USA) was utilized for

complementary DNA (cDNA) synthesis. DreamTaq Master Mix (ThermoScientific, Massachusetts, USA) and gene-specific primers (Table S1) were used to amplify the different date palm putative *PdGLX1* coding regions using the synthesized cDNA. These amplified genes were cloned into the pGEM-T Easy vector system (Promega, Wisconsin, USA), and the sequences were verified using the standard Sanger DNA sequencing method. The *attB1* and *attB2* sites were integrated using PCR and suitable oligonucleotides (Table S1) at the 5' and 3' end of each gene followed by the BP-clonase (Invitrogen, California, USA) reaction to generate the Gateway-entry clone pDONR-Zeo-PdGLX. Subsequently, the LR-clonase reaction (Invitrogen, California, USA) was used to sub-clone the genes into a bacterial expression vector pET-DEST42 (Invitrogen, California, USA) and into a yeast expression vector pYES-DEST52 (Invitrogen, California, USA). The Gateway cassette of pET-DEST42 vector was excised using the *BsrGI* restriction enzyme (ThermoScientific, Massachusetts, USA) and re-circularized using T4 ligase (NEB, Massachusetts, USA). This procedure has generated an empty vector, which was used as a negative control for subsequent experiments.

Expression profile of the *PdGLX1* gene family under stress conditions

The cDNA was synthesized using RNA extracted from the leaf and root tissues of date palm seedlings, as described earlier. This cDNA was used as a template to perform qPCR using Fast-SYBR (Invitrogen, California, USA) and gene-specific primers (Table S1) on the Biorad CFX96 Real-time PCR system (Biorad). The expression data were normalized to the expression of *ACTIN* as a reference gene⁴² and analyzed using the $2^{-\Delta\Delta CT}$ method.⁴³

Abiotic stress tolerance assay in *E. coli*

The bacterial expression cassettes pET-DEST42-PdGLX and empty pET-DEST42 were genetically transformed into BL21 *E. coli* cells using the Gene Pulser Xcell electroporation system (Bio-Rad, USA). The transgenic cells were cultured at 37°C in liquid LB containing 1 mg/ml ampicillin until they reach a mid-exponential growth phase ($OD_{600} \sim 0.6$). Subsequently, *PdGLX* gene expression was induced by the addition of 0.5 mM Isopropyl β -D-1-thiogalactopyranoside (IPTG) followed by treatment with the different stress inducers included salinity (250 mM NaCl), oxidative stress (5 mM H₂O₂), and MG toxicity (0.5 mM MG). The optical density (OD_{600}) was recorded at 2-hour intervals for a total growth period of 12 hours. The cells were then harvested to quantify the MG concentration. All measurements were conducted in three biological replicates.

Abiotic stress tolerance assay in yeast

The yeast expression cassettes pYES-DEST52-PdGLX and the empty pYES-DEST52 were transformed to MG hypersensitive yeast knockout GLO1 cell lines (YML004C; GLO1 BY4741; MAT a; his3 Δ 1; leu2 Δ 0; met15 Δ 0; ura3 Δ 0; YML004C::

kanMX4) (HVD Biotech Vertriebs Ges.m.b.H, Austria). The empty vector was also transformed into the wildtype yeast (*Saccharomyces cerevisiae*) parent strain (BY4741; MATa his3 Δ 1 leu2 Δ 0 met15 Δ 0 ura3 Δ 0) using a previously described PEG-lithium acetate heat shock method.⁴⁴ The transformed yeast knockout cells were then streaked on synthetically defined (SD)-agar plates with different concentrations of MG and incubated at 30°C for 72 h. Additionally, the transgenic yeast knockouts were cultured in SD glucose media until a mid-exponential growth phase ($OD_{600} \sim 0.8$), washed, and an equal number of cells were separately inoculated into SD galactose liquid media supplemented with the different stress conditions: 500 μ M MG, 700 μ M H₂O₂ and 500 mM NaCl. The growth of the cells was monitored spectrophotometrically (OD_{600}) at 6-h intervals for a total of 30 h and harvested for MG quantification at the 30-h time point.

MG quantification

The cellular MG level was estimated as previously described.⁴⁵ Briefly, the cells were harvested from liquid culture and lysed by suspension in 250 μ l of 5 M perchloric acid on ice for 15 min. The lysed cells were centrifuged at 11,000 g for 10 min, and the resultant supernatant was neutralized with 1 M Na₂HPO₄. The neutralized lysate was centrifuged at 11,000 g for 10 min, and 1 ml of the supernatant was transferred to a fresh tube, to which 10 μ l of NaN₃ was added. The concentration of MG in the cell lysate was quantified using a reaction mixture containing 650 μ l of the cell lysate, 250 μ l of 7.2 mM 1,2-diaminobenzene, and 100 μ l of 5 M perchloric acid. The absorbance was measured spectrophotometrically at 336 nm after 3 h incubation in the dark. The concentration of MG was calculated from an MG standard curve (1–100 μ M).

ROS accumulation in yeast cells

To evaluate the consequences of MG stress on ROS accumulation in yeast knockout GLO1 cells genetically transformed with the different expression cassettes (pYES-DEST52-PdGLX1), the transgenic yeast cells were grown until an early exponential stage ($OD_{600} \sim 0.6$) and harvested by centrifugation at room temperature. The cells were then treated with 0.5 mM MG for 7 h at 30°C, followed by staining with a peroxide-specific dye 50 mM 2',7'-dichlorodihydrofluorescein diacetate (H₂DCFAD) (Invitrogen, California, USA). The cells were also stained with a mitochondrial superoxide-specific dye 5 mM MitoSOX™ solution (Invitrogen, California, USA). The cells were stained in the dark for 30 min at 30°C, washed with phosphate buffer saline, and the ROS levels were determined by flow cytometry using the BD FACSAria™ flow cytometer (BD Biosciences, USA). The FlowJo software⁴⁶ was utilized to determine the mean fluorescent intensity (MFI) values from 5000 events.

Statistical analysis

One-way analysis of variance (ANOVA) and Dunnett's T3 post hoc test was used to compare the statistically significant differences between the mean of tested parameters against the control.

Statistical analyses were performed using the IBM SPSS statistical package version 21 (IBM Corp. Armonk, NY, USA).

Results

P. dactylifera L. genome encodes six *PdGLX1* genes

BLASTP search on the NCBI database against the date palm genome revealed a total of six putative *PdGLX1* genes from the genome of *P. dactylifera* L. Their sequence was then retrieved and further classified as *PdGLX1:1*, *PdGLX1:2*, *PdGLX1:3*, *PdGLX1:4*, *PdGLX1:5* and *PdGLX1:6* with the largest being *PdGLX1:4* with 1107 bp and the smallest being *PdGLX1:6* with 708 bp. Their locus location, gene identification number (id), mRNA identification number (id), protein identification number (id), coding sequences (CDS) length, and protein length are shown in Table S2.

Molecular phylogenetic analysis of the putative *PdGLX1* proteins was constructed using the Maximum Likelihood

method (ML). The percentage of trees in which the proteins clustered together is shown next to the branches based on 1000 bootstrap replicates (Figure 1a). Further, analyses of the coding region against the corresponding genomic sequence revealed the presence of eight introns in *PdGLX1:1*, *PdGLX1:3*, and *PdGLX1:4* genes. However, only seven introns were found in *PdGLX1:2*, *PdGLX1:5* and *PdGLX1:6* coding sequence in the *P. dactylifera* L. genome (Figure 1b).

The retrieved protein sequences were then searched for the presence of specific domains using the Hidden Markov Model (HMM) profile on the Pfam database. The results showed the presence of two Glyoxalase/Bleomycin resistance protein/Dioxygenase superfamily domain (PF00903.25) each for *PdGLX1:1–5*, which classifies these proteins as Ni²⁺-dependent GLX1 proteins, whereas *PdGLX1:6* has a single GLX1 domain and therefore classified as Zn²⁺-dependent GLX1 proteins. Together, the presence of these domains confirmed the identity of the retrieved sequences (Figure 2, Table S3).

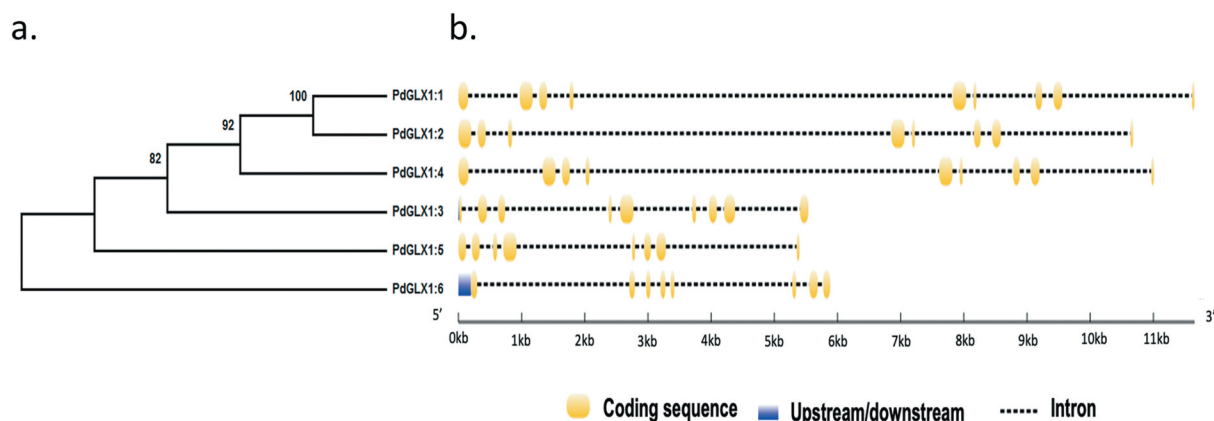


Figure 1. Phylogenetic analysis of the putative *PdGLX1* proteins using the Maximum Likelihood (ML) method (a). The percentage of trees in which the proteins clustered together is shown next to the branches based on 1000 bootstrap replicates. Intron-exon map of the different *PdGLX1* genes (b).

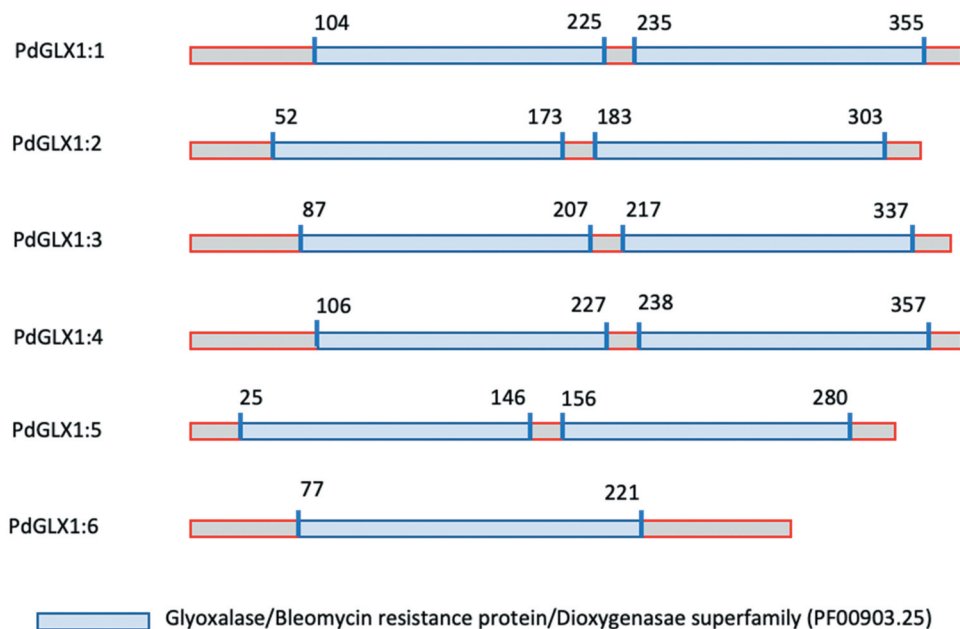


Figure 2. Domain architecture of the different *PdGLX1:1–6* proteins.

In-silico analysis of the molecular weight revealed that PdGLX1:4 had the largest molecular weight of 40.76 kDa, and PdGLX1:6 had the smallest molecular weight of 26.41 kDa. The results also showed that all the PdGLX1 proteins were acidic except PdGLX1:4, which was almost neutral (pI = 7.09), whereas the most acidic protein was PdGLX1:5 (pI = 5.17) (Table S4). Furthermore, computational subcellular localization prediction showed that all the putative PdGLX1 proteins were localized to the mitochondria, the chloroplast, and the cytosol using the PSORT and CELLO tools. Consistently, chloroplast transit peptides were also identified in the sequences of all the putative PdGLX1 proteins except for PdGLX1:5 proteins using the ChloroP localization tools (Table S4).

Analyses of the putative promoter sequences showed the presence of various *cis*-acting regulatory elements within 1.5 kb upstream of the *PdGLX1* start codon of the gene, including potential environmental stress and phytohormone transcription binding sites, suggesting that different environmental stimuli and phytohormones may regulate the expression of the *PdGLX1* genes (Table S5). Further, conserved motifs analysis using the MEME tool predicted the presence of various 7–8 bp conserved motifs with C/G rich regions, which may act as MG-responsive elements (Figure S1).

Multiple sequence analysis of the putative PdGLX1 proteins along with other previously well-characterized GLX1 orthologues from *Oryza sativa* and *Arabidopsis thaliana* showed that the GLX1 proteins are conserved. Besides, the Zn²⁺-dependent GLX1 proteins OsGLX1-8 and PdGLX1:6 had extended sequences which are labeled as A, B, and C (Figure 3). These

extra sequence stretches are characteristic of Zn²⁺-dependent GLY protein. In addition, the metal-binding sites were also identified and marked in triangles (Q/E/H/E), whereas the Ni²⁺-dependent GLX1 metal-binding sites (Q/E/Q/E) were also identified (Figure 3).

Conserved motif prediction using the MEME tool revealed the presence of various motifs from the retrieved protein sequences similar to those from *Arabidopsis thaliana* and *Oryza sativa* (Figure 4). The results showed that the motif 1 was shared among all the analyzed sequences. However, amino acid motifs 1–8 were common among all the Ni²⁺ dependent GLX1 proteins, while the Zn²⁺ dependent GLX1 proteins, AtGLX1-2, OsGLX1-8, and PdGLX1:6, had four identical motifs each. In addition, AtGLX1-6, PdGLX1:1, PdGLX1:2, PdGLX1:3, and PdGLX1:4 had nine identical motifs (Figure 4).

Phylogenetic analysis of the putative PdGLX1 and other protein orthologues of *Arabidopsis thaliana*, *Medicago sativa*, *Oryza sativa*, *Glycine max*, and *Sorghum bicolor* showed that the proteins were clustered into three major groups- Ni²⁺-dependent proteins (Clads I), Zn²⁺-dependent (Clade II) and GLX1-like proteins (Clade III). PdGLX1:1–5 proteins were all clustered into clade I, whereas PdGLX1:6 was clustered into clade II (Figure 5).

PdGLX1 genes were induced under different stress conditions

To examine the effect of different environmental stresses including saline (300 mM NaCl), oxidative (10 mM H₂O₂) and MG toxicity stresses (10 mM MG) on *PdGLX1* gene expression in the date palm seedlings, their expression profile

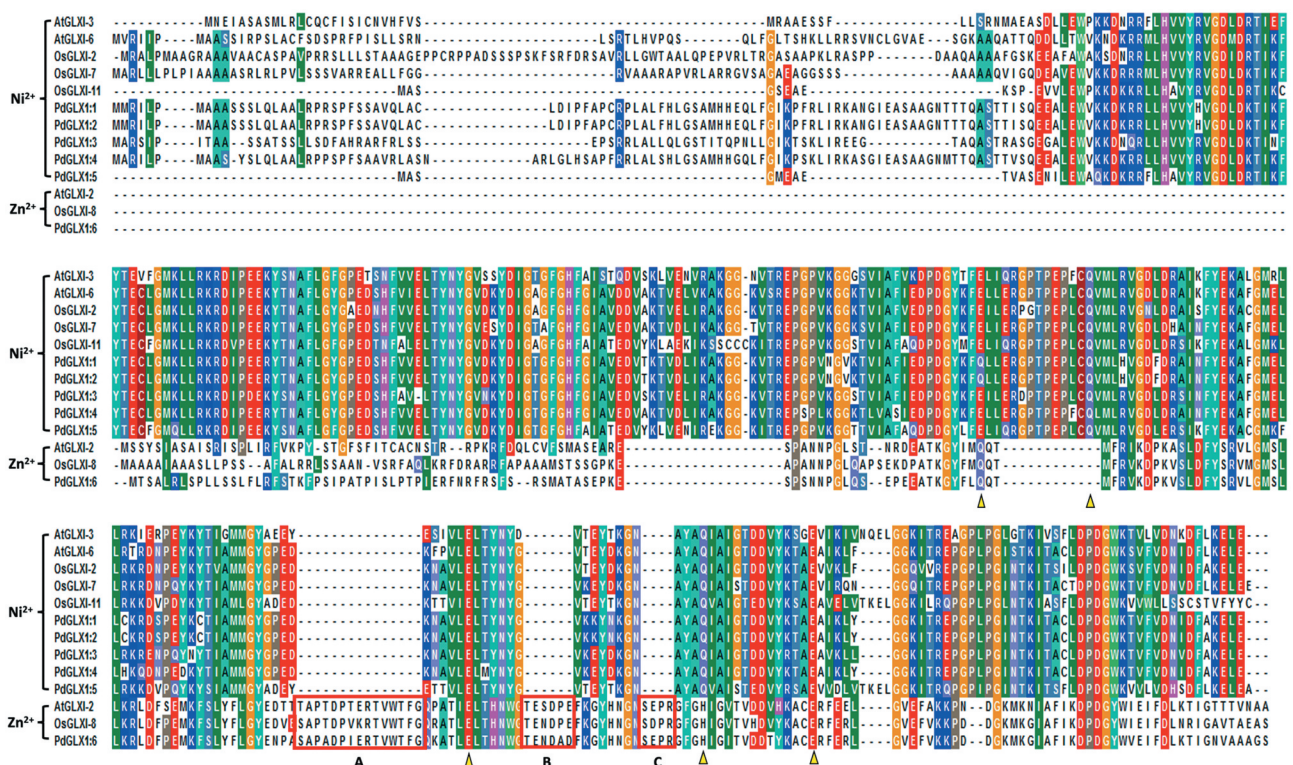


Figure 3. Multiple sequence analysis of the putative PdGLX1 proteins along with other previously well-characterized GLX1 orthologues from *Oryza sativa* and *Arabidopsis thaliana*. The Zn²⁺-dependent protein extended sequences are labeled as A, B, and C. Whereas, the Zn²⁺ (Q/E/H/E) and Ni²⁺ (Q/E/Q/E) metal-binding domain are shown in triangles.

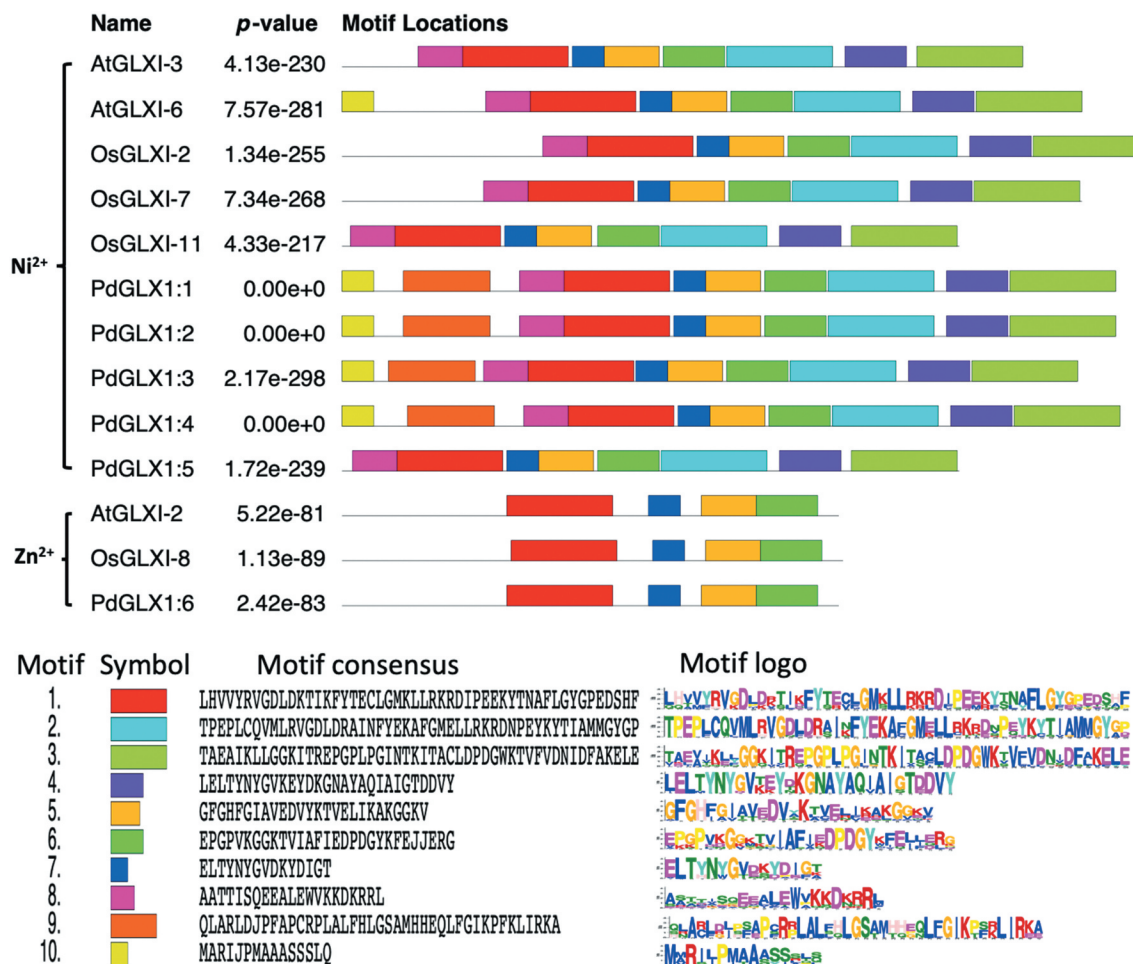


Figure 4. Conserved motifs identified by MEME of GLYOXALASE-I proteins identified from *Arabidopsis thaliana*, *Oryza sativa*, and *P. dactylifera* L. Lengths of motifs of each GLYOXALASE-I protein are displayed proportionally.

was analyzed using qPCR. The results showed that the expression of *PdGLX1* genes was altered depending on the stress in the leaf and root tissues (Figure 6). In general, there is a trend of upregulation of all the *PdGLX1* genes, with the expression of *PdGLX1:1* and *PdGLX1:4* being significantly ($p \leq 0.05$) upregulated under NaCl stress in leaf tissues, compared to the control treatment. However, the expression level of *PdGLX1:4* was reduced in the 10 mM H_2O_2 treated leaves. A similar trend of upregulation was observed in the root tissues of the treated plants, where the *PdGLX1:4* was significantly ($p \leq 0.05$) increased under H_2O_2 stress treatment. However, the expression of *PdGLX1:2*, *PdGLX1:3*, *PdGLX1:5*, and *PdGLX1:6* was not considerably altered under different stress treatments (Figure 6).

Heterologous expression of *PdGLX1* in *E. coli* confers tolerance to abiotic stresses

The *E. coli* BL21 cells transformed with the expression cassettes pET-DEST42-*PdGLX1:1-1:6* (Figure 7a) and the empty vector pET-DEST42 (as control) were grown in the presence of different abiotic stresses and the cultures were monitored spectrophotometrically (OD600). The growth of the transgenic *E. coli* cells increased significantly ($p \leq 0.001$) when compared with cells transformed with the empty vector under various abiotic

stress conditions such as 0.5 mM MG, 5 mM H_2O_2 and 250 mM NaCl (Figure 7b–d). In addition, the quantification of MG in the cells indicated a significant ($p \leq 0.001$) increase in the accumulation of MG in the empty control vector as compared to *E. coli* cells overexpressing the different *PdGLX1* genes under 0.5 mM MG (Figure 7b), 5 mM H_2O_2 (Figure 7c), and 250 mM NaCl (Figure 7d) stresses.

Overexpression of *PdGLX1* complements stress tolerance in knockout *GLO1 S. cerevisiae*

A complementation study of the MG-sensitive *GLO1* yeast cells transformed with expression cassettes pYES-DEST52-*PdGLX1:1-6* (Figure 8a) and empty vector pYES-DEST52 was conducted. To induce the expression of the *PdGLX1* transgene, the transgenic cells were streaked (Figure 8b) on Ura^- SD-galactose (Figure 8c) along with different concentrations of MG (Figure 8d–g). To block the expression of the *PdGLX1* within the construct and therefore, to verify its effect on the cells under various stresses, the transgenic cells were also streaked on Ura^- SD supplemented with glucose (Ura^- SD-glucose) (Figure 8h) along with different concentrations of MG (Figure 8i–j). The results of the complementation assays showed that the growth of the control yeast cells (transformed with empty vector) was impaired when Ura^- SD-galactose was

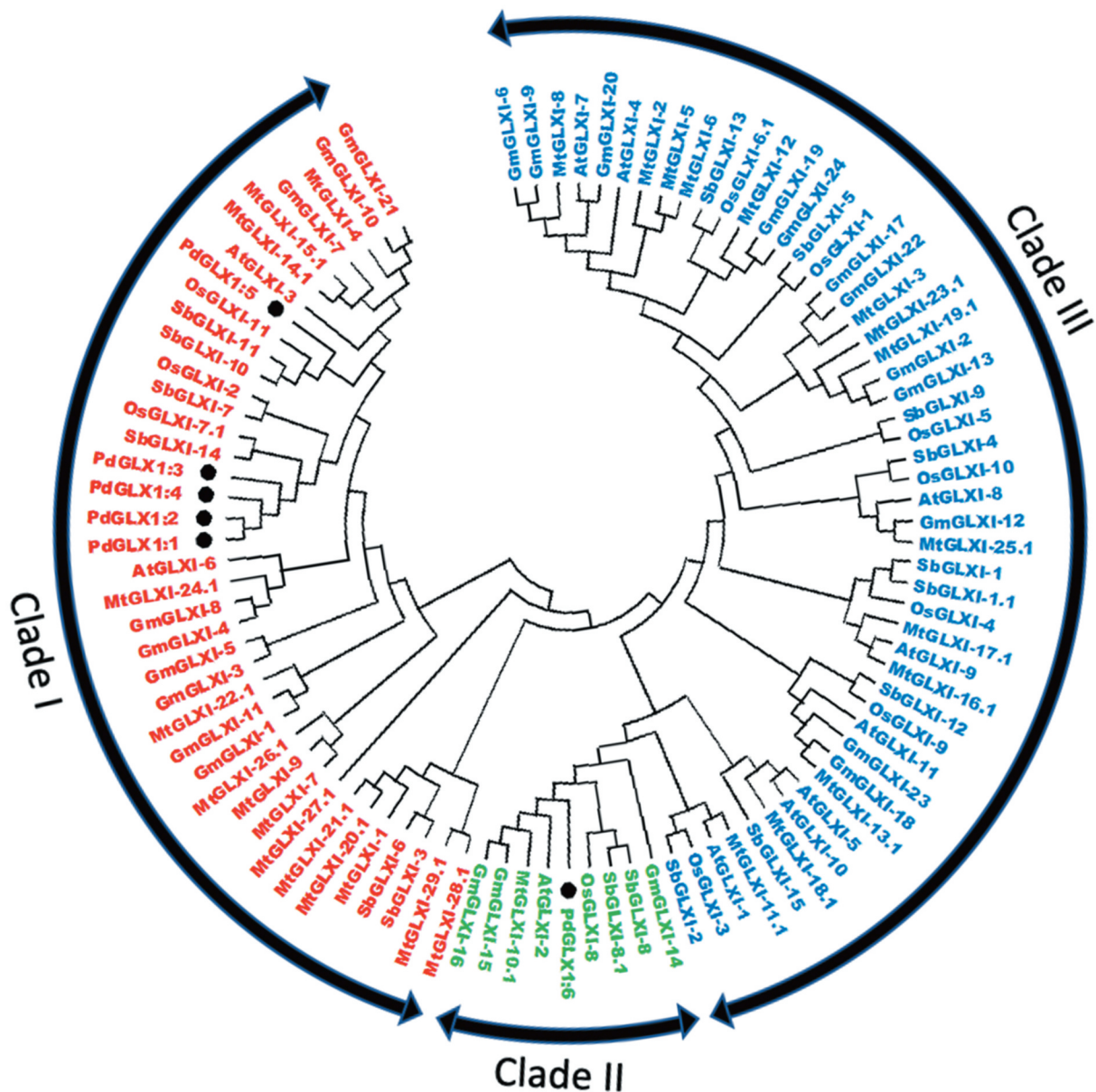


Figure 5. Phylogenetic analysis of Glyoxalase-I proteins identified from *P. dactylifera* L. and other plant species. Circular tree constructed for the GLXI proteins from *P. dactylifera* L., *Arabidopsis thaliana*, *Oryza sativa*, *Sorghum bicolor*, *Medicago sativa*, and *Glycine max* using Neighbor-Joining method in MEGA X with 1000 bootstrap replicates. The protein sequences are characterized as Clade I for Ni²⁺-dependent proteins, Clade II for Zn²⁺-dependent proteins, and Clade III for GLX-like proteins.

supplemented with 2 mM MG (Figure 8e). However, the growth was rescued when the yeast cells were transformed with the pYES-DEST52-*PdGLX1:1–6* expression cassettes. In addition, only the wild type BY4741 cells and the *PdGLX1:6* overexpressing GLO1 yeast knockouts were able to grow at 3 mM MG (Figure 8f) and 4 mM MG (Figure 8g). While the wildtype BY4741 cells were able to grow on the Ura⁻ SD-glucose plates supplemented with 1 mM and 2 mM MG, the knockout cells were unable to grow under the same conditions (Figure 8i–j).

Furthermore, the transgenic yeast cells were cultured in liquid SD-galactose along with the different abiotic stress inducers, and their growth was monitored spectrophotometrically (OD600) at 6 h intervals. The growth of the transgenic cells expressing the *PdGLX1* genes increased significantly ($p \leq 0.001$) compared to the cells transformed with an empty vector

under various abiotic stress conditions including 500 μ M MG (Figure 9a), 700 μ M H₂O₂ (Figure 9b) and 500 mM NaCl (Figure 9c). The cells transformed with the empty vector also indicated a significantly ($p \leq 0.001$) higher cellular accumulation of MG as compared to cells overexpressing the different *PdGLX1* genes under 500 μ M MG (Figure 9a), 700 μ M H₂O₂ (Figure 9b) and 500 mM NaCl conditions (Figure 9c).

Overexpression of *PdGLX1* in yeast reduced ROS accumulation

The accumulation of ROS in the transgenic yeast GLO1 knockout cell lines in response to the presence of 0.5 mM MG for seven hours was quantified by flow cytometry. The results revealed a significant reduction in cytosolic ROS accumulation

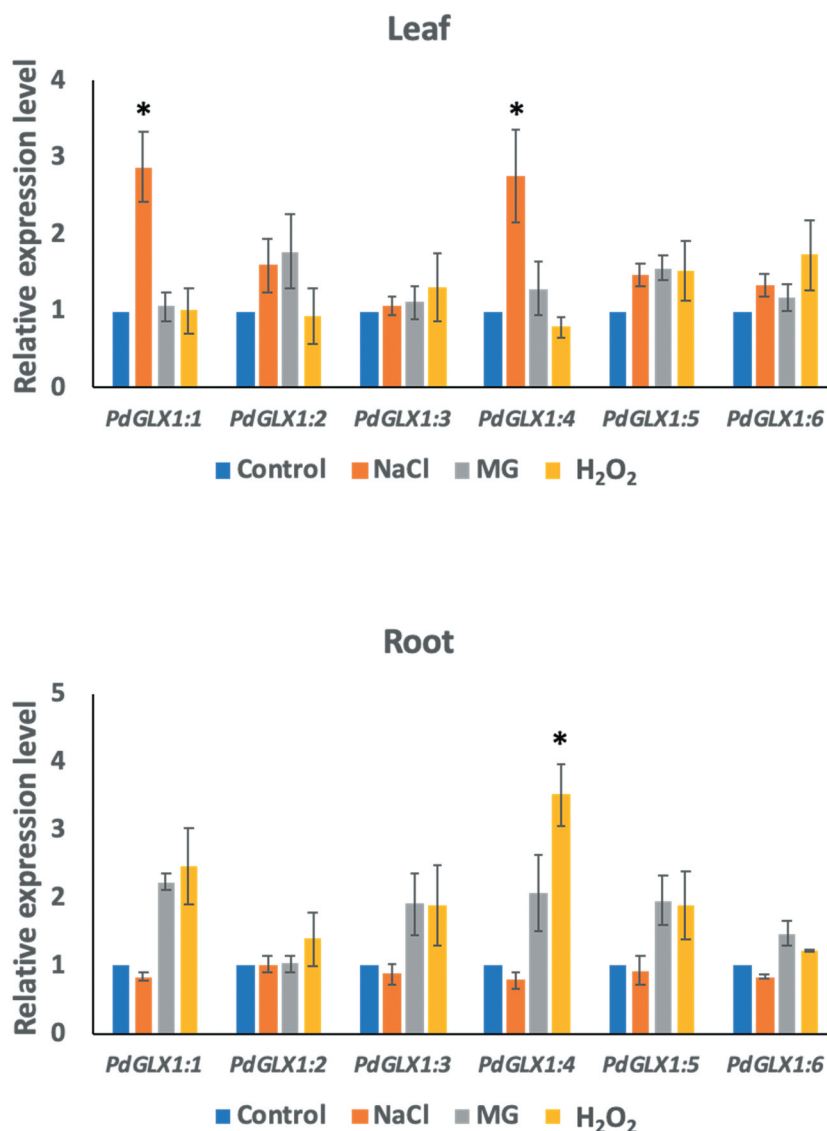


Figure 6. The relative expression level of the different *PdGLX1* genes in the leaf (a) and root (b) tissue using qPCR method. Asterisk (*) indicates $p \leq 0.05$; mean \pm SD, $n = 3$.

in the transgenic yeast cells with *PdGLX1:1*, *PdGLX1:4*, *PdGLX1:5* ($p \leq 0.001$) and *PdGLX1:6* ($p \leq 0.05$) genes as compared to knockout yeast cells transformed with the empty vector (Figure 10a). In addition, yeast cells transformed with *PdGLX1:2*, *PdGLX1:3*, and *PdGLX1:6* genes had a significant ($p \leq 0.05$) reduction in superoxide molecules in their mitochondria (Figure 10b).

Discussion

Plants sense and adapt their morphology, physiology, and gene expression under adverse environmental conditions by altering various stress signaling pathways to bring about cellular stability.⁴⁷ Different stress-associated signaling molecules have been identified in plants, which includes phytohormones,⁴⁸ ROS,⁴⁹ reactive nitrogen species (RNS)⁵⁰ and reactive carbonyl species (RCN).^{8,51} Studies have shown that ROS-mediated lipid peroxidation leads to the accumulation of RCN in plants.^{52,53} Among the RCN, MG has emerged

as an essential stress signaling molecule.⁸ MG is a by-product of numerous enzymatic and non-enzymatic reactions. It is a highly reactive cytotoxic metabolite, which accumulates in the cell under adverse environmental conditions leading to the inactivation of proteins, DNA, RNA, and lipids.^{12,24,51} To overcome the adverse effects of MG accumulation in the cell, various MG-detoxification mechanisms have been identified, of which the universally conserved glyoxalase system is the most efficient pathway involving two consecutive reactions catalyzed by GLXI and GLXII.^{10,20}

In silico analysis of the subcellular localization of the various putative *PdGLX1* proteins showed that the proteins are mainly localized to the cytosol, mitochondria, and chloroplast. In plants, ROS production is found mostly in the chloroplast, mitochondria, and peroxisome. Therefore, these sites may also be prone to ROS-mediated lipid peroxidation, which may lead to the accumulation of MG in these organelles.⁵⁴ In addition, the localization of the various putative *PdGLX1* proteins in the cytosol may help to keep a check on the level of MG

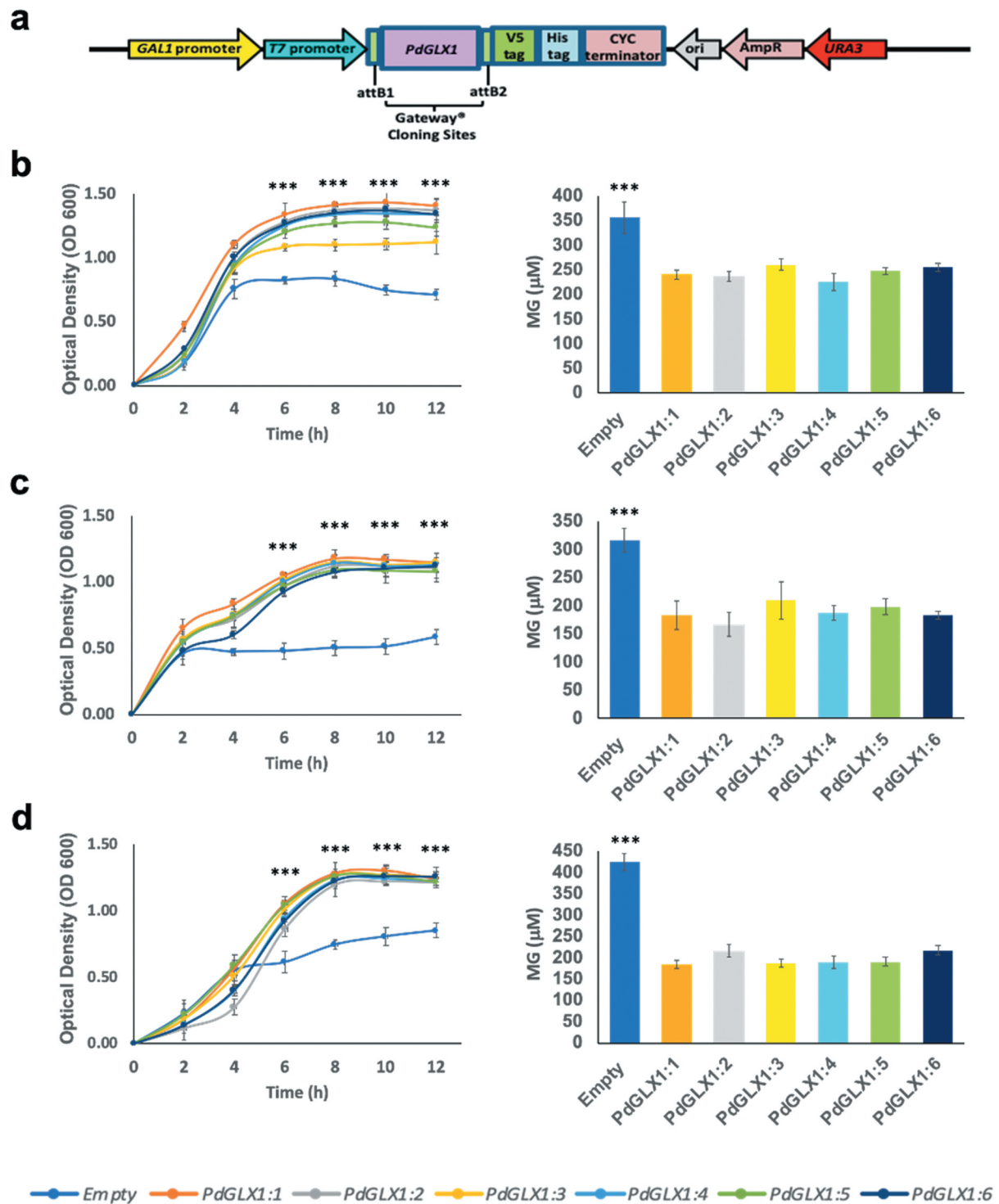


Figure 7. Heterologous expression of PdGLX1 enzymes in *E. coli* BL21 provides different levels of tolerance to various abiotic stresses. The PdGLX1 genes were cloned into the protein expression vector (pET-DEST52-PdGLX1:1–6) under the control of the T7 promoter (a). The transgenic bacteria were grown in the presence of different abiotic stresses, including MG (0.5 mM MG) (b), salinity (200 mM NaCl) (c), and oxidative stress (5 mM H₂O₂) (d). The MG concentration in the cells was measured for each treatment. The growth of the cells was spectrophotometrically monitored during the experiment. Asterisks (***) indicates $p \leq 0.001$; mean \pm SD, $n = 3$.

produced via glycolysis.⁵⁵ The localization of the putative PdGLX1 proteins to the chloroplast may suggest a mechanism to control the increasing level of MG originated mainly from the degradation of triose sugars via the Benson-Calvin cycle.⁵⁶ In the mitochondria, MG disrupts the electron transport chain and increases the generation of superoxide, NO, and peroxyntirite leading to mitochondrial oxidative

stress.⁵⁷ The localization of the various PdGLX1 proteins to the diverse organelles may suggest that the action of the putative PdGLX1 proteins is site-specific, and responds to different developmental stages and metabolic conditions induced by cellular and environmental changes as previously suggested.^{10,21} Further, promoter region analysis showed the presence of various potential environmental stresses and plant

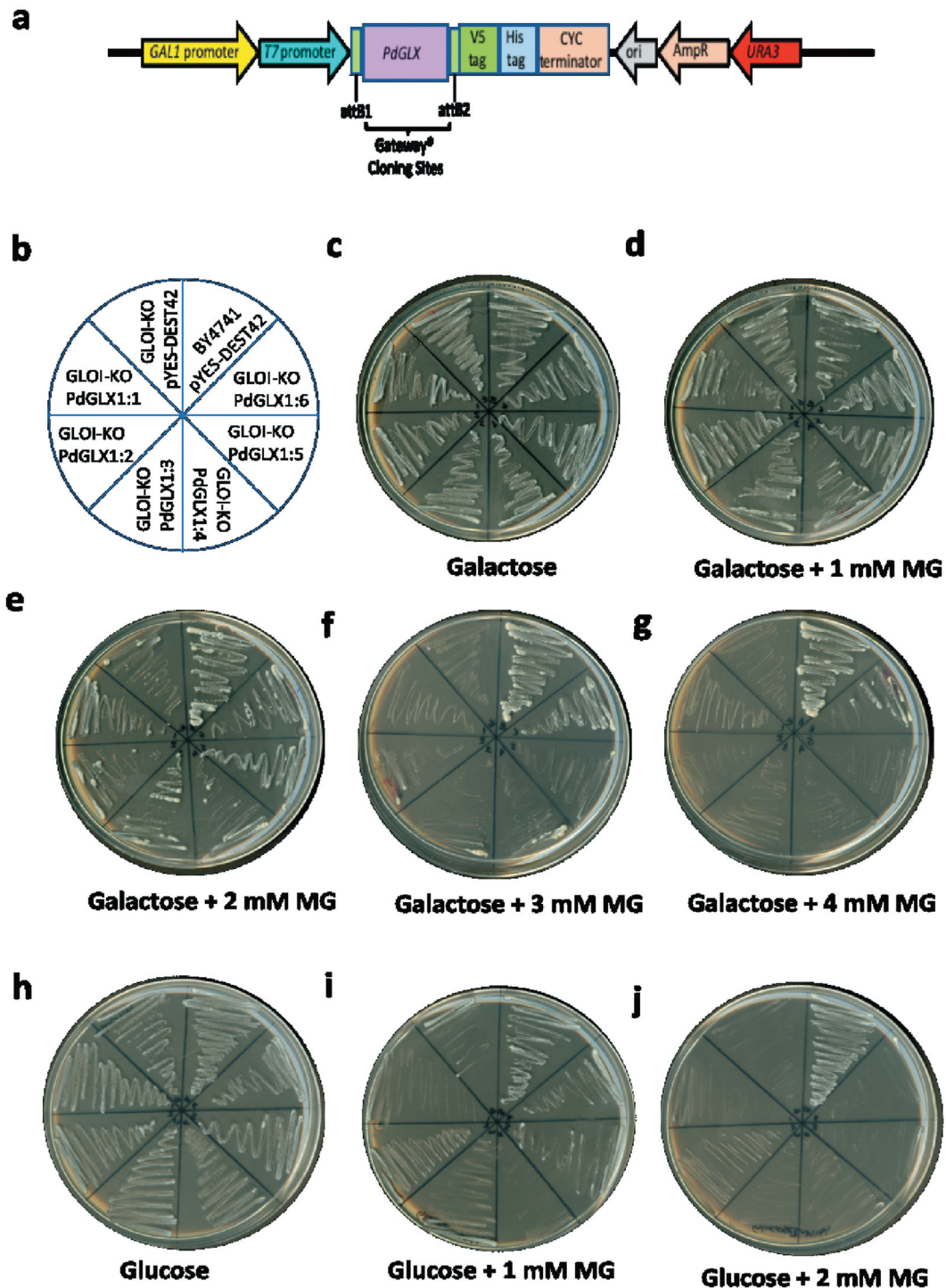


Figure 8. Mutant GLO1 yeast cells genetically transformed with the yeast expression cassette pYES-DEST52-*PdGLX1:1-6* (a). The pictorial representation of the different constructs are shown (b), the transgenic cells were then streaked on Ura⁻ SD galactose media (c), along with the different concentrations of MG; 1 mM MG (d), 2 mM MG (e), 3 mM MG (f), 4 mM MG (g), the transgenic cells were also streaked on different Ura⁻ SD glucose media (h), along with different concentrations of MG; 1 mM MG (i), 2 mM MG (j).

hormone activated transcription factors binding sites, suggesting that different environmental factors and hormones may regulate the expression of the *PdGLX1* genes. In addition, the identification of various 7–8 bp C/G rich conserved motifs upstream of the *PdGLX1* genes may suggest that these regions act as potential MG-responsive elements, as previously suggested.¹⁷

Glyoxalase-I is a metalloenzyme that requires divalent metal ions, such as Zn²⁺ or Ni²⁺ for its activity.⁵⁸ From the date palm genome, we identified both the Zn²⁺- and the Ni²⁺-dependent *PdGLX1* proteins based on the presence of the conserved domain sequences and the metal-binding domains. Further, the Zn²⁺- and Ni²⁺-dependent *PdGLX1* also differed in the presence of conserved motifs in their protein sequences. It has been previously suggested that the metal binding property of

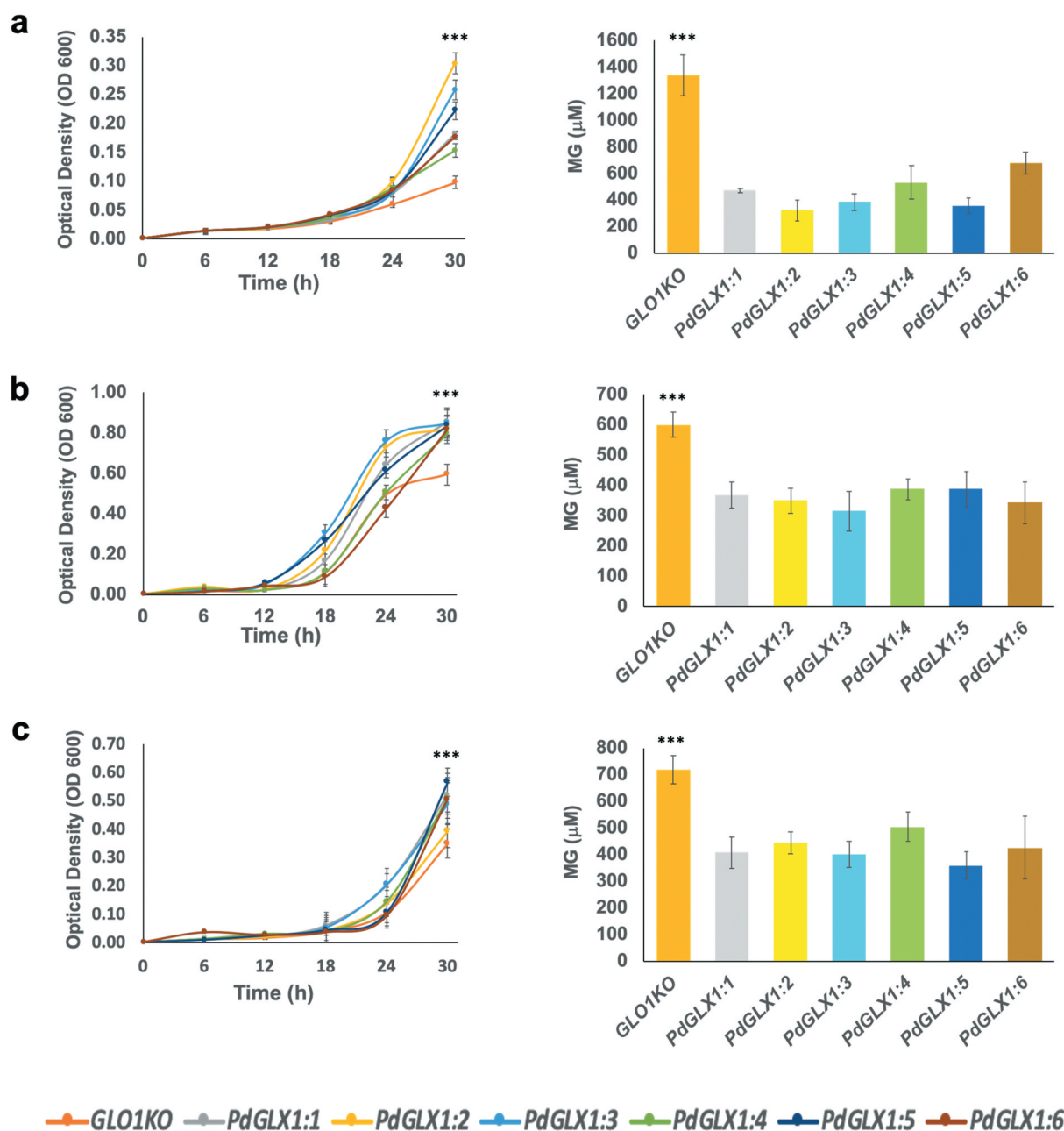


Figure 9. The growth of yeast mutant cells and the estimation of their MG content. The mutant GLO1 yeast cells genetically transformed with the yeast expression cassette pYES-DEST52-*PdGLX1:1–6* and the empty vector pYES-DEST52 were grown in liquid Ura⁻ SD galactose media in the presence of 500 μM MG (a), 700 μM H₂O₂ (b) and 500 mM NaCl (c). Asterisks (***) indicates $p \leq 0.001$; mean \pm SD, $n = 3$.

the GLX1 proteins can be identified based on the domain architecture of the proteins, where Zn²⁺ dependent proteins have a single larger domain (~140-142 amino acids) as compared to two smaller (~120 amino acids) conserved GLX1 domains found in the Ni²⁺ dependent GLX1 proteins. This notion is concurrent with our findings that the sequence of Zn²⁺ dependent PdGLX1:6 has a single conserved GLX1 domain as compared to the other Ni²⁺-dependent PdGLX1:1–5 proteins which have two conserved GLX1 domains.^{59,60} Further phylogenetic analysis of putative PdGLX1:1–6 proteins along with previously classified orthologs from *Arabidopsis thaliana*, *Medicago sativa*, *Oryza sativa*, *Glycine max* and *Sorghum bicolor*⁶¹ show that PdGLX1:1–5

were classified in the (Clade I) Ni²⁺ dependent GLX1 proteins whereas PdGLX1:6 was grouped into the (Clade II) Zn²⁺ dependent GLX1 proteins.

Gene expression analysis showed an increasing trend of *PdGLX1* expression under the tested stress conditions. The differential expression of these genes appears to be tissue-specific under various environmental stresses since we observed a significant upregulation of the *PdGLX1:1* and *PdGLX1:4* genes in the leaf tissue in response to 300 mM NaCl stress, whereas there was no change in their expression in the root tissues under the same conditions. However, there was a trend of upregulation of the *PdGLX1* genes in the root tissue in response to the H₂O₂ and MG stress treatment. In

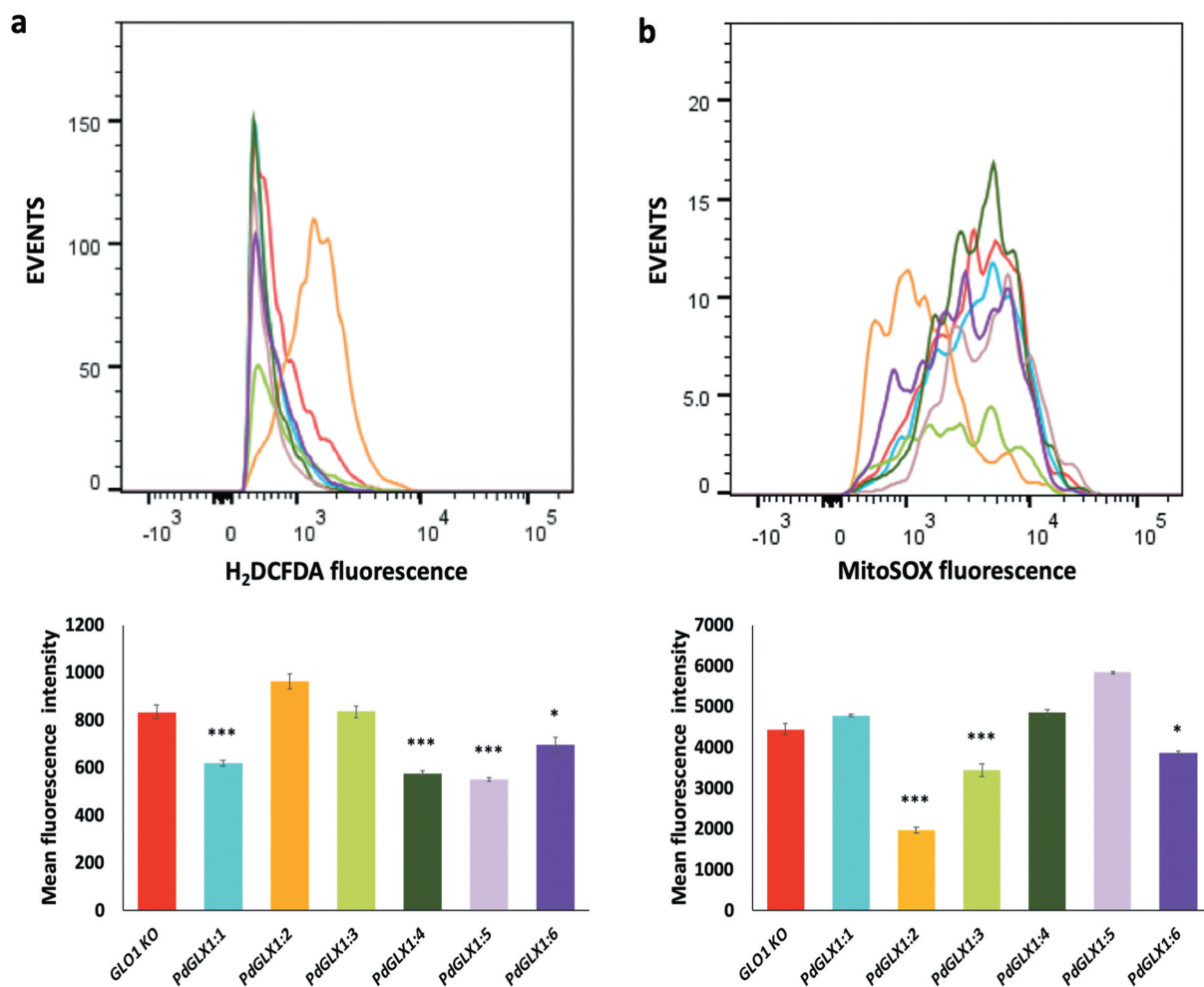


Figure 10. ROS quantification by flow cytometry in GLO1 mutant cells transformed with *PdGLX1* genes or the empty negative control vector. The cells were stained to detect cytosolic ROS accumulation using H₂DCFAD stain (a) or the mitochondria specific superoxide using the MitoSOX™ stain (b). Graphs indicate the mean fluorescent intensity (5000 events). Asterisks (***) indicates $p \leq 0.001$, Asterisk (*) indicates $p \leq 0.05$; mean \pm SD, $n = 3$.

line with these observations, various reports have previously shown that there is an increase in the levels of MG and the expression of the MG detoxification *GLX1* genes under stress conditions.^{13,62} Furthermore, the importance of the *GLX1* genes in enhancing stress tolerance has been verified by transgenic overexpression of *GLX1* genes in numerous crop plants such as tobacco,^{29,63} black gram,⁶⁴ rice,⁶⁵ pumpkin²³ and sugar beet.²⁸ Therefore, the overexpression of the putative *PdGLX1* genes under the tested conditions implies a stress tolerance mechanism in date palm to maintain MG at a nontoxic level.

Heterologous expression of the putative *PdGLX1* genes in *E. coli* cells significantly enhanced their growth and reduced MG accumulation. This observation can be attributed to the ability of the PdGLX1 proteins to enhance the glyoxalase system in the cells, which is the main route of MG detoxification in bacteria.⁶⁶ Moreover, it is consistent with previous reports indicating that various stress conditions lead to the accumulation of MG, which in turn hinders the growth of bacteria.^{67–69} Our conclusions are also supported by previous findings showing that overexpression of the Arabidopsis *GLY1* confers stress tolerance to *E. coli* cells.⁴⁵

In yeast, the detoxification of MG is controlled by the *GLO1* and *GRE3* genes. Therefore, mutant yeast cells lacking *PdGLX1* genes were sensitive to exogenous application of MG and showed a higher cellular accumulation of MG due to the loss of function of the *GLO1* gene.⁷⁰ In the present study, the yeast complementation assay showed that the *PdGLX1* genes were able to complement the loss in function of the MG-sensitive GLO1 knockout yeast cell line genetically transformed with *PdGLX1:1–6*. These transgenic yeast cells displayed normal growth in Ura⁻SD-galactose supplemented with high MG concentration, whereas the growth of the empty vector control cells was hindered even at a low MG concentration. The *PdGLX1* genes were cloned under the control of the *GAL1*-promoter, which is activated by galactose and suppressed by glucose. Therefore, the enhanced growth was not observed when the transgenic GLO1 cells were streaked on Ura⁻SD-glucose supplemented with low concentrations of MG. This test showed that *PdGLX1* genes are responsible for enhancing the growth of the GLO1 knockout yeast. Among the different overexpressing PdGLX1:1–6 GLO1 knockout yeast cell lines, the overexpression of the Zn²⁺-dependent Glyoxalase-I protein PdGLX1:6 showed enhanced survival of the GLO1 knockout lines on Ura⁻SD-galactose plates supplemented with high MG

concentration. This finding may suggest a greater efficiency of the Zn²⁺-dependent protein than that of the Ni²⁺-dependent protein in the detoxification of MG, which is consistent with previous studies in other plant species.⁷¹ Further, overexpressing the putative *PdGLX1* genes enhanced not only the MG-detoxification activity but also the antioxidant activity and, hence the salinity stress tolerance of the GLO1 knockouts mutants.

Cumulatively, our observations imply that the PdGLX1 protein family can catalyze MG detoxification and maintain the cellular redox balance in the date palm, thus enabling its growth under various stress conditions. Future experimental works, including overexpression and localization of *PdGLX1* genes *in planta*, are needed to understand better the MG detoxification and antioxidant mechanisms conferred by *PdGLX1* genes in date palm.

Acknowledgments

Authors would like to acknowledge the College of Science, Sultan Qaboos University, Oman, for the generous fund number IG/SCI/BIOL/18/01 to MWY. The authors would like to thank Dr. Sirin Adham, Sultan Qaboos University, for her help in the flow cytometry, which was used in this study.

Disclosure of Potential Conflicts of Interest

The authors declare that they have no conflict of interest. All authors revised and approved the final manuscript.

Funding

This work was supported by the Sultan Qaboos University [IG/SCI/BIOL/18/01].

ORCID

Gerry Aplang Jana  <http://orcid.org/0000-0002-0314-2392>
Mahmoud W. Yaish  <http://orcid.org/0000-0002-5171-3014>

Authors' contributions

GAJ conceived, designed, performed the experiments, analyzed data, and wrote the manuscript, and MWY designed the experiments, supervised the work, edited the manuscript, and contributed reagents/materials/analysis tools.

References

- Assaha DV, Ueda A, Saneoka H, Al-Yahyai R, Yaish MW. The role of Na⁺ and K⁺ transporters in salt stress adaptation in glycophytes. *Front Physiol.* 2017;8:509. doi:10.3389/fphys.2017.00509.
- Atkinson NJ, Urwin PE. The interaction of plant biotic and abiotic stresses: from genes to the field. *J Exp Bot.* 2012;63(10):3523–3543. doi:10.1093/jxb/ers100.
- Jana GA, Al Kharusi L, Sunkar R, Al-Yahyai R, Yaish MW. Metabolomic analysis of date palm seedlings exposed to salinity and silicon treatments. *Plant Signal Behav.* 2019;14(11):1663112. doi:10.1080/15592324.2019.1663112.
- Yaish MW, Kumar P. Salt tolerance research in date palm tree (*Phoenix dactylifera* L.). *Front Plant Sci.* 2015;6:348.
- Al-Harrasi I, Patankar HV, Al-Yahyai R, Sunkar R, Krishnamurthy P, Kumar PP, Yaish MW. Molecular characterization of a date palm vascular highway 1-interacting kinase (PdVIK) under abiotic stresses. *Genes.* 2020;11(5):568. doi:10.3390/genes11050568.
- Al-Harrasi I, Jana GA, Patankar HV, Al-Yahyai R, Rajappa S, Kumar PP, Yaish MW. A novel tonoplast Na⁺/H⁺ antiporter gene from date palm (PdNHX6) confers enhanced salt tolerance response in *Arabidopsis*. *Plant Cell Rep.* 2020;39(8):1079–1093. doi:10.1007/s00299-020-02549-5.
- Jana GA, Yaish MW. Genome-wide identification and functional characterization of glutathione peroxidase genes in date palm (*Phoenix dactylifera* L.) under stress conditions. *Plant Gene.* 2020;23:100237. doi:10.1016/j.plgene.2020.100237.
- Hoque TS, Hossain MA, Mostofa MG, Burritt DJ, Fujita M, Tran L-SP. Methylglyoxal: an emerging signaling molecule in plant abiotic stress responses and tolerance. *Front Plant Sci.* 2016;7:1341. doi:10.3389/fpls.2016.01341.
- Sharma R, De Vleeschauwer D, Sharma MK, Ronald PC. Recent advances in dissecting stress-regulatory crosstalk in rice. *Mol Plant.* 2013;6(2):250–260. doi:10.1093/mp/sss147.
- Schmitz J, Dittmar IC, Brockmann JD, Schmidt M, Hüdig M, Rossoni AW, Maurino VG. Defense against reactive carbonyl species involves at least three subcellular compartments where individual components of the system respond to cellular sugar status. *Plant Cell.* 2017;29(12):3234–3254. doi:10.1105/tpc.17.00258.
- Saito R, Yamamoto H, Makino A, Sugimoto T, Miyake C. Methylglyoxal functions as Hill oxidant and stimulates the photo-reduction of O₂ at photosystem I: a symptom of plant diabetes. *Plant Cell Environ.* 2011;34(9):1454–1464. doi:10.1111/j.1365-3040.2011.02344.x.
- Kaur C, Singla-Pareek SL, Sopory SK. Glyoxalase and methylglyoxal as biomarkers for plant stress tolerance. *CRC Crit Rev Plant Sci.* 2014;33(6):429–456. doi:10.1080/07352689.2014.904147.
- Yadav SK, Singla-Pareek SL, Ray M, Reddy MK, Sopory SK. Methylglyoxal levels in plants under salinity stress are dependent on glyoxalase I and glutathione. *Biochem Biophys Res Commun.* 2005a;337(1):61–67. doi:10.1016/j.bbrc.2005.08.263.
- Cai Y-T, Zhang H, Qi Y-P, Ye X, Huang Z-R, Guo J-X, Chen L-S, Yang L-T. Responses of reactive oxygen species and methylglyoxal metabolisms to magnesium-deficiency differ greatly among the roots upper and lower leaves of *Citrus sinensis*. *BMC Plant Biol.* 2019;19:76.
- Hoque TS, Uraji M, Tuya A, Nakamura Y, Murata Y. Methylglyoxal inhibits seed germination and root elongation and up-regulates transcription of stress-responsive genes in ABA-dependent pathway in *Arabidopsis*. *Plant Biol.* 2012c;14(5):854–858. doi:10.1111/j.1438-8677.2012.00607.x.
- Hoque TS, Okuma E, Uraji M, Furuichi T, Sasaki T, Hoque MA, Nakamura Y, Murata Y. Inhibitory effects of methylglyoxal on light-induced stomatal opening and inward K⁺ channel activity in *Arabidopsis*. *Biosci Biotechnol Biochem.* 2012b;76(3):617–619. doi:10.1271/bbb.110885.
- Kaur C, Kushwaha HR, Mustafiz A, Pareek A, Sopory SK, Singla-Pareek SL. Analysis of global gene expression profile of rice in response to methylglyoxal indicates its possible role as a stress signal molecule. *Front Plant Sci.* 2015a;6:682. doi:10.3389/fpls.2015.00682.
- Hoque MA, Uraji M, Torii A, Banu MNA, Mori IC, Nakamura Y, Murata Y. Methylglyoxal inhibition of cytosolic ascorbate peroxidase from *Nicotiana tabacum*. *J Biochem Mol Toxicol.* 2012a;26(8):315–321. doi:10.1002/jbt.21423.
- Kaur C, Sharma S, Singla-Pareek SL, Sopory SK. Methylglyoxal, triose phosphate isomerase, and glyoxalase pathway: implications in abiotic stress and signaling in plants. In: Pandey G. (eds) *Elucidation of abiotic stress signaling in plants*. Springer; 2015. p. 347–366. https://doi.org/10.1007/978-1-4939-2211-6_13
- Álvarez Viveros MF, Inostroza-Blancheteau C, Timmermann T, González M, Arce-johnson P. Overexpression of GlyI and GlyII genes in transgenic tomato (*Solanum lycopersicum* Mill.) plants confers salt tolerance by decreasing oxidative stress. *Mol Biol Rep.* 2013;40(4):3281–3290. doi:10.1007/s11033-012-2403-4.

21. Kaur C, Sharma S, Singla-Pareek SL, Sopory SK. Methylglyoxal detoxification in plants: role of glyoxalase pathway. *Indian J Plant Physiol.* 2016;21(4):377–390. doi:10.1007/s40502-016-0260-1.
22. Hossain MA, Hasanuzzaman M, Fujita M. Up-regulation of anti-oxidant and glyoxalase systems by exogenous glycinebetaine and proline in mung bean confer tolerance to cadmium stress. *Physiol Mol Biol Plants.* 2010;16(3):259–272. doi:10.1007/s12298-010-0028-4.
23. Hossain MA, Hossain MZ, Fujita M. Stress-induced changes of methylglyoxal level and glyoxalase I activity in pumpkin seedlings and cDNA cloning of glyoxalase I gene. *Aust J Crop Sci.* 2009;3:53.
24. Li Z-G. Methylglyoxal and glyoxalase system in plants: old players, new concepts. *Bot Rev.* 2016;82(2):183–203. doi:10.1007/s12229-016-9167-9.
25. Mustafiz A, Singh AK, Pareek A, Sopory SK, Singla-Pareek SL. Genome-wide analysis of rice and Arabidopsis identifies two glyoxalase genes that are highly expressed in abiotic stresses. *Funct Integr Genomics.* 2011;11(2):293–305. doi:10.1007/s10142-010-0203-2.
26. Singla-Pareek S, Reddy M, Sopory S. Genetic engineering of the glyoxalase pathway in tobacco leads to enhanced salinity tolerance. *Proc Natl Acad Sci.* 2003;100(25):14672–14677. doi:10.1073/pnas.2034667100.
27. Veena RVS, Sopory SK. Glyoxalase I from Brassica juncea: molecular cloning, regulation and its over-expression confer tolerance in transgenic tobacco under stress. *Plant J.* 1999;17(4):385–395. doi:10.1046/j.1365-313X.1999.00390.x.
28. Wu C, Ma C, Pan Y, Gong S, Zhao C, Chen S, Li H. Sugar beet M14 glyoxalase I gene can enhance plant tolerance to abiotic stresses. *J Plant Res.* 2013;126(3):415–425. doi:10.1007/s10265-012-0532-4.
29. Yadav SK, Singla-Pareek SL, Reddy MK, Sopory SK. Transgenic tobacco plants overexpressing glyoxalase enzymes resist an increase in methylglyoxal and maintain higher reduced glutathione levels under salinity stress. *FEBS Lett.* 2005b;579(27):6265–6271. doi:10.1016/j.febslet.2005.10.006.
30. Yaish MW, Patankar HV, Assaha DV, Zheng Y, Al-Yahyai R, Sunkar R. Genome-wide expression profiling in leaves and roots of date palm (*Phoenix dactylifera* L.) exposed to salinity. *BMC Genomics.* 2017;18(1):246. doi:10.1186/s12864-017-3633-6.
31. Yaish MW, Sunkar R, Zheng Y, Ji B, Al-Yahyai R, Sardar FA. A genome-wide identification of the miRNAome in response to salinity stress in date palm (*Phoenix dactylifera* L.). *Front Plant Sci.* 2015;6(946). doi:10.3389/fpls.2015.00946.
32. Eddy SR. Profile hidden Markov models. *Bioinformatics.* 1998;14(9):755–763. doi:10.1093/bioinformatics/14.9.755.
33. Bjellqvist B, Hughes GJ, Pasquali C, Paquet N, Ravier F, Sanchez JC, Frutiger S, Hochstrasser D. The focusing positions of polypeptides in immobilized pH gradients can be predicted from their amino acid sequences. *Electrophoresis.* 1993;14(1):1023–1031. doi:10.1002/elps.11501401163.
34. Horton P, Park K-J, Obayashi T, Fujita N, Harada H, Adams-Collier C, Nakai K. WoLF PSORT: protein localization predictor. *Nucleic Acids Res.* 2007;35(suppl_2):W585–W587. doi:10.1093/nar/gkm259.
35. Yu CS, Chen YC, Lu CH, Hwang JK. Prediction of protein sub-cellular localization. *Proteins: structure.* 2006;64(3):643–651. doi:10.1002/prot.21018.
36. Emanuelsson O, Nielsen H, Von Heijne G. ChloroP, a neural network-based method for predicting chloroplast transit peptides and their cleavage sites. *Protein Sci.* 1999;8(5):978–984. doi:10.1110/ps.8.5.978.
37. Lescot M, Déhais P, Thijs G, Marchal K, Moreau Y, Van de Peer Y, Rouzé P, Rombauts S. PlantCARE, a database of plant cis-acting regulatory elements and a portal to tools for in silico analysis of promoter sequences. *Nucleic Acids Res.* 2002;30(1):325–327. doi:10.1093/nar/30.1.325.
38. Hu B, Jin J, Guo A-Y, Zhang H, Luo J, Gao G. GSDS 2.0: an upgraded gene feature visualization server. *Bioinformatics.* 2014;31(8):1296–1297. doi:10.1093/bioinformatics/btu817.
39. Bailey TL, Johnson J, Grant CE, Noble WS. The MEME suite. *Nucleic Acids Res.* 2015;43(W1):W39–W49. doi:10.1093/nar/gkv416.
40. Kumar S, Stecher G, Li M, Knyaz C, Tamura K. MEGA X: molecular evolutionary genetics analysis across computing platforms. *Mol Biol Evol.* 2018;35(6):1547–1549. doi:10.1093/molbev/msy096.
41. Xiao Y, Yang Y, Cao H, Fan H, Ma Z, Lei X, Mason AS, Xia Z, Huang X. Efficient isolation of high quality RNA from tropical palms for RNA-seq analysis. *Plant Omics.* 2012;5:584.
42. Patankar HV, Assaha DV, Al-Yahyai R, Sunkar R, Yaish MW. Identification of reference genes for quantitative real-time PCR in date palm (*Phoenix dactylifera* L.) subjected to drought and salinity. *PLoS One.* 2016;11(11):e0166216. doi:10.1371/journal.pone.0166216.
43. Livak KJ, Schmittgen TD. Analysis of relative gene expression data using real-time quantitative PCR and the 2⁻ΔΔCT method. *Methods.* 2001;25(4):402–408. doi:10.1006/meth.2001.1262.
44. Schiestl RH, Gietz RD. High efficiency transformation of intact yeast cells using single stranded nucleic acids as a carrier. *Curr Genet.* 1989;16(5–6):339–346. doi:10.1007/BF00340712.
45. Jain M, Nagar P, Sharma A, Batth R, Aggarwal S, Kumari S, Mustafiz A. GLYI and D-LDH play key role in methylglyoxal detoxification and abiotic stress tolerance. *Sci Rep.* 2018;8(1):5451. doi:10.1038/s41598-018-23806-4.
46. Becton D (2019) FlowJo™ Software. 10.5.3 edn.
47. Zhu J-K. Abiotic stress signaling and responses in plants. *Cell.* 2016;167(2):313–324. doi:10.1016/j.cell.2016.08.029.
48. Verma V, Ravindran P, Kumar PP. Plant hormone-mediated regulation of stress responses. *BMC Plant Biol.* 2016;16(1):86. doi:10.1186/s12870-016-0771-y.
49. Choudhury S, Panda P, Sahoo L, Panda SK. Reactive oxygen species signaling in plants under abiotic stress. *Plant Signal Behav.* 2013;8(4):e23681. doi:10.4161/psb.23681.
50. Luis A, Sandalio LM, Corpas FJ, Palma JM, Barroso JB. Reactive oxygen species and reactive nitrogen species in peroxisomes. Production scavenging, and role in cell signaling. *Plant Physiol.* 2006;141:330–335.
51. Mostofa MG, Ghosh A, Li Z-G, Siddiqui MN, Fujita M, Tran L-SP. Methylglyoxal—a signaling molecule in plant abiotic stress responses. *Free Radic Biol Med.* 2018;122:96–109. doi:10.1016/j.freeradbiomed.2018.03.009.
52. Biswas MS, Mano J. Lipid peroxide-derived short-chain carbonyls mediate hydrogen peroxide-induced and salt-induced programmed cell death in plants. *Plant Physiol.* 2015;168(3):885–898. doi:10.1104/pp.115.256834.
53. Mano J. Reactive carbonyl species: their production from lipid peroxides, action in environmental stress, and the detoxification mechanism. *Plant Physiol Biochem.* 2012;59:90–97. doi:10.1016/j.plaphy.2012.03.010.
54. Das K, Roychoudhury A. Reactive oxygen species (ROS) and response of antioxidants as ROS-scavengers during environmental stress in plants. *Front Environ Sci.* 2014;2:53. doi:10.3389/fenvs.2014.00053.
55. Plaxton WC. The organization and regulation of plant glycolysis. *Ann Rev Plant Physiol Plant Mol Biol.* 1996;47(1):185–214. doi:10.1146/annurev.arplant.47.1.185.
56. Takagi D, Inoue H, Odawara M, Shimakawa G, Miyake C. The calvin cycle inevitably produces sugar-derived reactive carbonyl methylglyoxal during photosynthesis: a potential cause of plant diabetes. *Plant Cell Physiol.* 2014;55(2):333–340. doi:10.1093/pcp/pcu007.
57. Hossain MA, Teixeira da Silva J, Fujita M. Glyoxalase system and reactive oxygen species detoxification system in plant abiotic stress response and tolerance: an intimate relationship. *Abiotic Stress.* 2011;1:235–266.
58. Jain M, Batth R, Kumari S, Mustafiz A. Arabidopsis thaliana contains both Ni²⁺ and Zn²⁺ dependent glyoxalase I enzymes and ectopic expression of the latter contributes more towards abiotic stress tolerance in *E. coli*. *PLoS One.* 2016;11(7):7. doi:10.1371/journal.pone.0159348.

59. Kaur C, Sharma S, Hasan MR, Pareek A, Singla-Pareek SL, Sopory SK. Characteristic variations and similarities in biochemical, molecular, and functional properties of glyoxalases across prokaryotes and eukaryotes. *Int J Mol Sci.* 2017;18(4):250. doi:10.3390/ijms18040250.
60. Li T, Cheng X, Wang Y, Yin X, Li Z, Liu R, Liu G, Wang Y, Xu Y. Genome-wide analysis of glyoxalase-like gene families in grape (*Vitis vinifera* L.) and their expression profiling in response to downy mildew infection. *BMC Genomics.* 2019;20(1):362. doi:10.1186/s12864-019-5733-y.
61. Bhowal B, Singla-Pareek SL, Sopory SK, Kaur C. From methylglyoxal to pyruvate: a genome-wide study for the identification of glyoxalases and D-lactate dehydrogenases in *Sorghum bicolor*. *BMC Genomics.* 2020;21(1):145. doi:10.1186/s12864-020-6547-7.
62. Espartero J, Sánchez-Aguayo I, Pardo JM. Molecular characterization of glyoxalase-I from a higher plant; upregulation by stress. *Plant Mol Biol.* 1995;29(6):1223–1233. doi:10.1007/BF00020464.
63. Singla-Pareek SL, Yadav SK, Pareek A, Reddy M, Sopory S. Transgenic tobacco overexpressing glyoxalase pathway enzymes grow and set viable seeds in zinc-spiked soils. *Plant Physiol.* 2006;140(2):613–623. doi:10.1104/pp.105.073734.
64. Bhomkar P, Upadhyay CP, Saxena M, Muthusamy A, Prakash NS, Pooggin M, Hohn T, Sarin NB. Salt stress alleviation in transgenic *Vigna mungo* L. Hepper (blackgram) by overexpression of the glyoxalase I gene using a novel *Cestrum* yellow leaf curling virus (CmYLCV) promoter. *Mol Breeding.* 2008;22(2):169–181. doi:10.1007/s11032-008-9164-8.
65. Zeng Z, Xiong F, Yu X, Gong X, Luo J, Jiang Y, Kuang H, Gao B, Niu X, Liu Y. Overexpression of a glyoxalase gene, OsGly I, improves abiotic stress tolerance and grain yield in rice (*Oryza sativa* L.). *Plant Physiol Biochem.* 2016;109:62–71. doi:10.1016/j.plaphy.2016.09.006.
66. Ferguson GP, Töttemeyer S, MacLean M, Booth IR. Methylglyoxal production in bacteria: suicide or survival? *Arch Microbiol.* 1998;170(4):209–218. doi:10.1007/s002030050635.
67. Campbell AK, Naseem R, Holland IB, Matthews SB, Wann KT. Methylglyoxal and other carbohydrate metabolites induce lanthanum-sensitive Ca²⁺ transients and inhibit growth in *E. coli*. *Arch Biochem Biophys.* 2007;468(1):107–113. doi:10.1016/j.abb.2007.09.006.
68. Cooper R. Metabolism of methylglyoxal in microorganisms. *Ann Rev Microbiol.* 1984;38(1):49–68. doi:10.1146/annurev.mi.38.100184.000405.
69. Inoue Y, Kimura A. Methylglyoxal and regulation of its metabolism in microorganisms. In: RK. Poole (Ed.) *Advances in microbial physiology.* Vol. 37. Elsevier; 1995. p. 177–227. [https://doi.org/10.1016/S0065-2911\(08\)60146-0](https://doi.org/10.1016/S0065-2911(08)60146-0)
70. Aguilera J, Antonio Prieto J. Yeast cells display a regulatory mechanism in response to methylglyoxal. *FEMS Yeast Res.* 2004;4(6):633–641. doi:10.1016/j.femsyr.2003.12.007.
71. Batth R, Jain M, Kumar A, Nagar P, Kumari S, Mustafiz A. Zn²⁺-dependent glyoxalase I plays the major role in methylglyoxal detoxification and salinity stress tolerance in plants. *Plos One.* 2020;15(5):e0233493. doi:10.1371/journal.pone.0233493.